

Identification of Precursor Species in the Formation of MFI Zeolite in the TPAOH–TEOS–H₂O System

Christine E. A. Kirschhock, Raman Ravishankar, Frederik Verspeurt, Piet J. Grobet, Pierre A. Jacobs, and Johan A. Martens*

Centrum voor Oppervlaktechemie en Katalyse, K.U. Leuven, Kardinaal Mercierlaan 92, B-3001, Heverlee, Belgium

Received: January 25, 1999; In Final Form: March 28, 1999

²⁹Si liquid NMR and in situ infrared spectroscopy was used to investigate the polycondensation process of tetraethyl orthosilicate (TEOS) in a concentrated aqueous solution of tetrapropylammonium hydroxide (TPAOH) at low temperatures. The composition was characterized by a molar hydrolysis ratio (H₂O/TEOS) of 6 and a molar TPAOH/TEOS ratio of 0.37. The ²⁹Si NMR spectra and the infrared spectra of the samples recorded at different reaction times and temperatures were assigned to a limited number of specific silicate polyanions containing three and five rings. The structure directing action of tetrapropylammonium cations was evidenced by the formation of silicate polyanions with a curved hydrophobic SiO₂ surface, such as the bicyclic pentamer, pentacyclic octamer, and the tetracyclic undecamer. At room temperature, the polycondensation process leads to the selective formation of a species containing 33 Si atoms. It occluded a tetrapropylammonium molecule and had the same framework connectivity as in bulk MFI zeolite. This TEOS polycondensation process may be relevant for the first steps of the crystallization of MFI type zeolites.

Introduction

Zeolites represent a continuously growing family of natural and synthetic microporous crystalline oxide materials with different framework structures, chemical compositions, crystal sizes, and morphologies.¹ The large variety of presently known synthetic zeolite topologies has been realized by making use of organic template molecules, acting as guest species in the zeolite pores during the crystallization processes and controlling pore shape and dimensions. Organic template molecules thus play a key role in the kinetics and thermodynamics of the zeolite crystallization process.² The detailed molecular mechanisms of nucleation and growth of zeolite crystals and the effect of templates on these processes remain unclear. In recent ²⁹Si NMR studies on tetraalkylammonium silicate solutions,^{3,4} Kinrade et al. demonstrated the tremendous influence of these templates on the formation of polysilicate anions. The smaller alkyl groups, as in tetramethylammonium, direct the system toward small, closed, cage-like structures, whereas the larger alkyl chains favor the formation of more open structures.

Zeolites with the MFI framework topology are members of the pentasil family which have in common that their framework structures are built from five-membered rings.⁵ The MFI type SiO₂ polymorph, known as Silicalite-1, can be crystallized from a relatively simple mixture of tetrapropylammonium hydroxide (TPAOH) acting as template, a silicon source, and water.⁶ Many authors have investigated the interaction of tetrapropylammonium cations with silica hydrogels or solutions.^{3,4,7–15} It is generally believed that the template is responsible for the formation of oligomeric silicate precursor species that later form the final MFI framework. A preference for the formation of five-ring species in TPAOH–silicate mixtures was shown,⁷ and small five-ring containing species such as the double five-ring^{8,9}

or the capped double five-ring¹⁰ were discussed as precursors. Other authors claimed fragments of the MFI framework as essential intermediates. The tetrapod^{11,12} or the channel cross-section¹³ may serve as examples. These have in common that the embryonic particle already contains template molecules and therewith can account for the selective formation of MFI zeolites in the presence of TPAOH.

In the previous work,¹⁴ we reported the formation of a specific nanoslab with dimensions of 1.3 × 4.0 × 4.0 nm as the end product of the polycondensation process at room temperature. These nanoslabs were proposed to already have the MFI topology and occluded TPA in channel intersections. Thus, the search for possible precursor species has to be made at earlier stages, namely, between the initial contact of TEOS with concentrated TPAOH and before the formation of these nanoslabs, which occurs upon dilution with water and aging at room temperature. Therefore, TEOS was hydrolyzed in concentrated TPAOH solution at 0 °C and at room temperature and the silicon polycondensation process was followed using ²⁹Si liquid NMR and IR spectroscopy. With this approach, we succeeded in identification of the initially formed polycondensation products from TEOS in contact with the template and were able to come up with a molecular model explaining why the MFI structure is selectively built when using TPAOH as a template.

Experimental Section

Concentrated aqueous TPAOH solution (Fluka, 40%) and TEOS (Acros, 98%) were mixed according to a molar hydrolysis ratio (H₂O/TEOS) of 6 and a TPAOH/SiO₂ ratio of 0.37.

The procedure of extraction of the silicate species from solution involved a sequence of acidification, salting out, phase transfer into organic solvent, and freeze-drying and was explained in the previous article.¹⁴

In situ FTIR experiments were performed on a Nicolet 730 instrument. The samples were introduced as a droplet in a

* Corresponding author telephone, 0032-16-321637; fax, 0032-16-321998; e-mail, johan.martens@agr.kuleuven.ac.be.

mirrored cup in a DRIFT setup at room temperature. A small volume of TPAOH solution was introduced into the probe volume and an equal amount of TEOS was carefully added on top of it. The sample environment was flushed with dry nitrogen. The background was recorded before and after each set of measurements and subtracted from the spectra. Pure TEOS and TPAOH solution served as reference samples. The evolution of the sample was monitored by accumulation of 16 spectra every five minutes between 1 and 46 min after the first contact of TEOS and TPAOH. After this time, no further significant changes could be observed. This procedure was repeated several times to optimize the experimental parameters and to ensure reproducibility.

Spectra of extracted solid material in KBr pellets were recorded with the same spectrometer in the transmission mode.

^{29}Si liquid NMR was performed on a Bruker AMX 300 MHz (7 T) at 0 °C. Block decays were accumulated with pulse lengths of 4 μs (45° pulse) and repeating times of 10 s. Between 5000 and 8000 spectra were accumulated. The samples were transferred into a cylindrical PTFE sample container surrounding a thin PTFE tube containing TMS as standard. Short test measurements before and after the main accumulation were taken to make sure the samples were stable during the long times of scanning. Several experiments were duplicated to verify reproducibility.

Intensity ratios and chemical shifts were determined with the Winfit software (Bruker). In the discussion of the chemical shifts, only the first two decimals are mentioned.

Results and discussion

IR. IR spectra were recorded in time after adding a droplet of TEOS to a droplet of concentrated aqueous TPAOH solution at room temperature in a DRIFT setup (Figure 1A). Distinct absorptions appear in the regions between 500 and 700 cm^{-1} and 1000–1100 cm^{-1} . As soon as TEOS is added to TPAOH solution, a sharp band at 650 cm^{-1} is observed. This band decreases in intensity in favor of a broad band centered first at 600 cm^{-1} , shifting later towards lower wavenumbers. A further band at 1050 cm^{-1} gains intensity during the whole experiment. As the latter signal corresponds to an asymmetric stretching of the Si–O–Si bond in silicates,^{16,17} its gain in intensity proves the progress of the silicon condensation process. The final IR spectrum closely resembles MFI-type zeolite, although the band at 590 cm^{-1} is displaced from the one usually observed at 550 cm^{-1} . In literature, the latter band has been specifically assigned to five-ring structures in pentasil zeolites.¹⁸ The frequency shift can be ascribed to the small size of the silicate molecule containing the five rings, and the lack of connectivity of the five rings with a framework. The evolution of this five-ring vibration, depending on the particle size, is illustrated in Figure 1B with solids extracted during the course of crystallization of Silicalite-1 from these solutions. Material extracted from mixtures of TEOS and concentrated TPAOH aged at room temperature (indicated as “precursor”) exhibits an IR spectrum that is very similar to the one observed at the end of the in situ experiment (Figure 1A), both having a band at 590 cm^{-1} . Nanoslab particles, measuring $1.3 \times 4 \times 4$ nm and which form upon dilution of this aged, concentrated TEOS–TPAOH mixture,¹⁴ are characterized by a band at 570 cm^{-1} (Figure 1Bb).¹⁹ The final colloidal Silicalite-1 material obtained after 5 days heating at 100 °C and with particle size of 18–100 nm displays a split band with maxima at 570 and 550 cm^{-1} .²⁰ Bulk micron size MFI-type material⁶ shows the characteristic signal at 550 cm^{-1} (Figure 1Bc). It is inferred that the signal initially

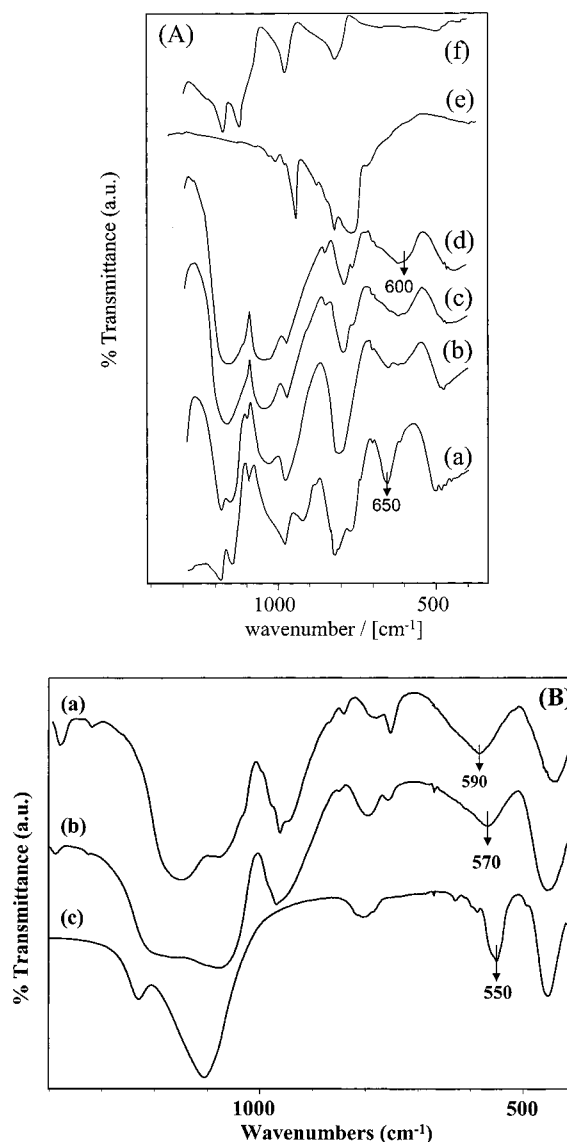


Figure 1. (A) In situ IR spectra of TPAOH–TEOS mixture after time intervals of: (a) 1 min, (b) 10 min, (c) 20 min, and (d) 46 min, respectively, (e) TEOS, and (f) TPAOH. (B) IR spectra of extracted solids: (a) precursor, (b) nanoslab, and (c) micron size Silicalite-1.⁶

TABLE 1: Samples Investigated with ^{29}Si NMR

sample	S1		S2	
mixing time (min)	15	45	15	45
mixing temperature (°C)	0	0	20	20
phase separation	yes	yes	yes	no
measurement temperature (°C)	0	0 and 20	0	0

observed at 600 cm^{-1} is a feature of the MFI type of connectivity, and especially of the arrangement of five rings. As will be shown later, ^{29}Si liquid NMR gives evidence for the presence of three-ring species after short times. Therefore, the sharp band at 650 cm^{-1} can be assigned to three-ring units. This also is in accordance with the trend that rings with decreasing size vibrate at higher frequencies.^{16,17}

NMR. Samples were prepared by adding 9 g TEOS to 7.9 g of concentrated TPAOH solution, either at room temperature (r.t.) or 0 °C. The mixture was intensively agitated with a magnetic stir bar to provoke hydrolysis of the silicon source. An overview of reaction times and temperatures is provided in Table 1. During mixing, the samples behaved as an unstable emulsion of TEOS in the aqueous TPAOH phase. Interruption

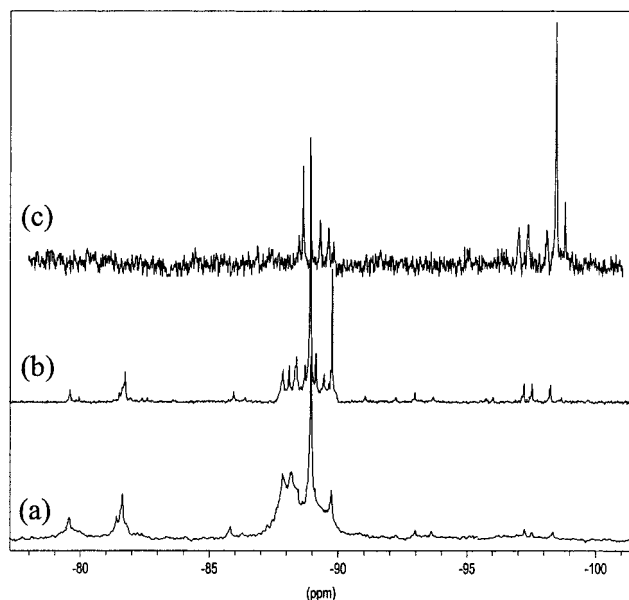


Figure 2. ^{29}Si NMR spectra of the sample prepared at 0 °C and stirred for (a) 10 min, (b) 15 min, and (c) 45 min.

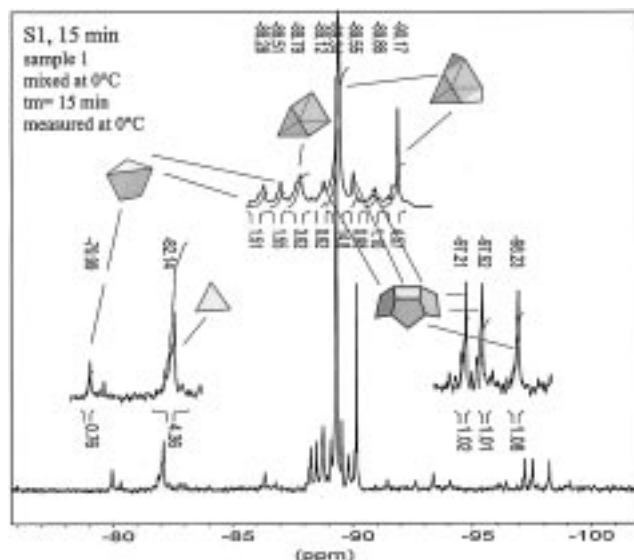


Figure 3. Assigned ^{29}Si NMR spectrum of the sample prepared at 0 °C after 15 min stirring.

of the stirring resulted in a phase separation, except for the S2, 45 min sample, for which a homogeneous phase was obtained. The aqueous layer was separated from the organic TEOS layer and washed with octane solvent to remove unreacted TEOS. The washing procedure also was applied to the S2, 45 min sample. ^{29}Si liquid NMR investigation of the organic layer and the octane extract proved both to contain only TEOS as the Si atom containing molecule in significant amounts. Upon storage of the samples at 0 °C there were no changes of the NMR spectra. Thus, it was possible to investigate the evolution of silicon species in this system by running ^{29}Si liquid NMR on the aqueous phases. The evolution of the ^{29}Si NMR spectrum with time is illustrated for the 0 °C system in Figure 2. Assigned representative spectra prepared at 0 °C, r.t., and different stirring times are given in Figures 3–7.

At first sight, the NMR spectra recorded after different reaction times at the two temperatures (Figures 2–7) appear quite complex. A comparative analysis of a large number of spectra allows identification of sets of lines always having the

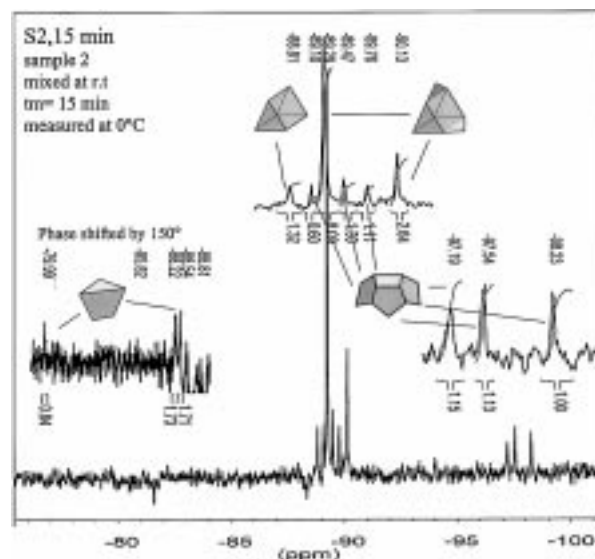


Figure 4. Assigned ^{29}Si NMR spectrum of the sample prepared at 0 °C after 45 min stirring.

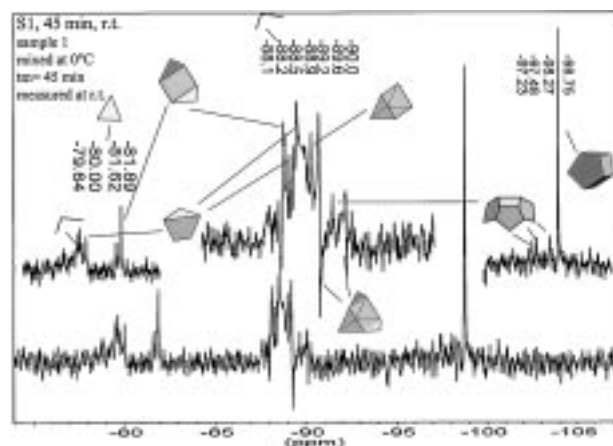


Figure 5. Assigned ^{29}Si NMR spectrum of the sample of Figure 3 subsequently heated in the spectrometer to room temperature.

same intensity ratios but different overall intensities. Each group of signals is assumed to stem from a specific entity present in the mixture. In some spectra, a group of signals exhibit a phase shift (e.g., S2, 15 min; S1, 45 min, r.t., Figures 5 and 6). It turned out that the samples contained variable amounts of residual octane from the TEOS extraction procedure. The latter was found to be responsible for the phase shift observation. The organic solvent was found to selectively interact with small silicate entities in these mixtures, thus providing a different environment than the aqueous solution. The detection of these phase shifts proved to be fortunate because the signals shifted in phase can directly be considered as belonging to one molecular species. The grouping of signals in four representative samples is given in Figure 8. Graphical representations of the silicate species and their chemical shifts in the different samples and according to literature are provided in Figure 9.

The lines at $\delta = -82.15$ ppm in S1, 15 min and $\delta = -81.63$ ppm in S1, 45 min and the line at ca. $\delta = -88.8$ ppm lacking any correlation in intensity to other signals are assigned to the single three-ring, and the double three-ring, respectively, on the basis of chemical shifts from literature^{21,22} (Figure 9). Three additional lines at $\delta = -80.00$, -88.51 , and -88.28 ppm, respectively, always appearing in the ratio of 1:2:2, are identified with the bicyclic pentamer in accordance with chemical shifts

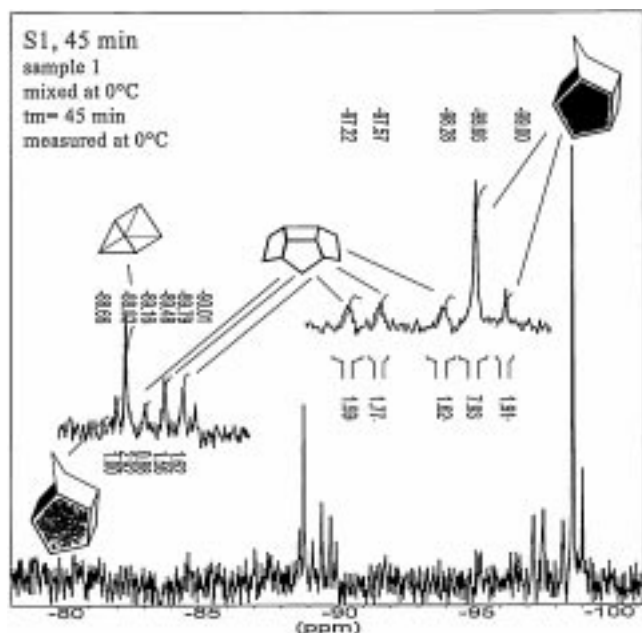


Figure 6. Assigned ^{29}Si NMR spectrum of the sample prepared at room temperature after stirring for 15 min.

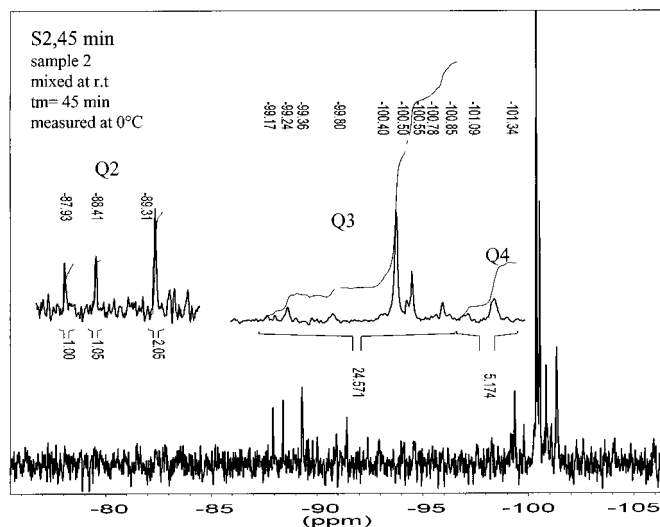


Figure 7. ^{29}Si NMR spectrum of the sample prepared at room temperature and stirred for 45 min.

from literature²¹ (Figure 9). Besides these three entities, only two more groups of lines are observed in samples S1, 15 min and S2, 15 min (Figures 3, 6, and 8). The two lines at ca. $\delta = -89.3$ and -90.2 ppm, respectively, with intensity ratio of 3:1, dominate both spectra. Both signals appear in the region of Q^2 and Q^3 in highly condensed three-ring containing structures.²¹ The shifts of the Q^3 atoms, specifically, coincide with the respective shifts in the pentacyclic heptamer, but the observed intensity ratio is in disagreement with this assignment. In the work of Harris and Knight, the signal of the Q^2 silicon of this molecule was not observed.²³ This can be explained by taking into account the possibility of coincidence of the shifts of the Q^2 and one of the Q^3 nuclei. The pentacyclic octamer has the same atomic environments as the described pentacyclic heptamer and fits the intensity ratio 3:1 when Q^2a and Q^3b (Figure 9) give rise to a same shift. The structure of the pentacyclic octamer corresponds to two annealed five-rings that are doubly bridged and can be obtained by condensation of the bicyclic pentamer and a three-ring, which are simultaneously present (Figures 3, 5, and 6).

S1, 15 min ppm I_{rel}	S2, 15 min ppm I_{rel}	S1, 45 min ppm I_{rel}	S1, 45 min, r.t. ppm
-80.0 0.76	-80.0 0.84*		-79.6
			-80.0
			-81.6
			-81.9
-82.2 4.36			
-88.3 1.51	-88.2 1.71*		-88.3
-88.5 1.55	-88.5 1.73*		-88.6
		-88.7 1	
-88.8 3.62	-88.8 1.32	-88.8 2.92	-88.9
-89.1 0.62	-89.1 0.60	-89.2 0.88	
-89.3 14.8	-89.3 5.09		-89.2
-89.6 0.98	-89.6 1.30	-89.6 1.56	a)
-89.8 1.10	-89.8 1.11	-89.8 1.62	-89.6
-90.1 4.57	-90.1 2.64		-90
-97.2 1.02	-97.2 1.15	-97.2 1.59	-97.2
-97.5 1.01	-97.5 1.13	-97.6 1.77	-97.5
-98.2 1.08	-98.2 1	-98.3 1.62	-98.3
		-98.7 7.93	
			-98.8
		99 1.91	

Figure 8. Chemical shifts and relative signal intensities in samples S1, 15 min; S2, 15 min; S1, 45 min; and S1, 45 min, r.t. Signals belonging to the same species are grouped. Concise determination of the chemical shift of signals (marked by "a") is difficult because of neighboring signals with phase shift (marked by an asterisk).

The last species in the S1 and S2, 15 min samples gives rise to six signals, three in the Q^3 and three in the Q^2 regions (Figures 3 and 6). The intensity ratio of 2:2:2:2:2:1 speaks for an entity with either a mirror plane or a 2-fold axis with one Q^2 atom falling on the symmetry element. With the information from the IR experiment that five rings are present in large numbers, only one silicon atom arrangement matching the symmetry requirements is possible. The proposed tetracyclic undecamer can be described as three annealed five-rings with a connection of the two outermost rings (Figure 9). This half cage-like structure can be built by the condensation of a pentacyclic octamer with a three-ring species. Thus, the decrease of the concentration of these smaller entities in the later recorded NMR spectra (S1 and S2, 45 min, Figures 4 and 7) and the retreat of the IR band at 650 cm^{-1} assigned to three-rings (Figure 1A) can be accounted for.

The observation of only a few species and especially an open structure like the tetracyclic undecamer is at first quite surprising. The preference for the formation of five-rings such as the double five-ring has been reported earlier,⁷ but those studies always resulted in observation of a vast variety of highly condensed and relatively small species. Contrary to the present study, the previous work was concerned with mixtures containing alkali metal cations and excessive water in addition to TEOS and TPA. The formation of the open structure of the tetracyclic undecamer can, therefore, directly be ascribed to a structure directing effect of the template, clearly evidenced in these concentrated solutions.

Pentacyclic octamer and tetracyclic undecamer are the largest entities formed during the first 15 min at room temperature and at 0°C (Figures 3 and 6). The further evolution of the mixture depends on the temperature. After 45 min at 0°C (S1, 45 min, Figure 4), two new intense lines appear at $\delta = -98.67$ and -99.18 ppm, respectively, as well as a new signal in the Q^2 region ($\delta = -88.66$ ppm). The same sample measured after subsequent heating to room temperature in the spectrometer (S1, 45 min r.t., Figure 5) is dominated by a single strong line at $\delta = -98.75$ ppm, identified as the double five-ring.²¹ The




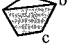





								
Three-ring	Tricyclic hexamer	Double three ring	Bicyclic pentamer	Pentacyclic octamer	Tetracyclic undecamer (Monomer)	33-mer (Trimer)	Capped double five ring	Double five ring
S1, 15 min 82.15 S1,45min,r.t. 81.63 lit. 81.43	S1,45min,r.t. a: 81.90 b: 88.11 lit.: a: 81.80 b: 88.10	S1, 15 min 88.79 S2, 15 min 88.81 S1, 45 min 88.83 S1,45min,r.t. "-88.9" lit. 88.38	S1, 15 min a: 80.00 b: 88.51 c: 88.28 a:b:c 1:2.03:1.97 S2, 15 min a: 80.00 b: 88.54 c: 88.22 a:b:c 1:2.02:2.05 S1,45min,r.t. lit. a: 80.00 b: 88.54 c: 88.30 lit. a: 81.16 b: 88.41 c: 87.58	S1, 15 min a,b: 89.34 c: 90.18 (a+b):c 3.24:1 S2,15 min a,b: 89.30 c: 90.13 (a+b):c 3.07:1 S1,45min,r.t. a,b:"89.24" c:"90.10" lit.** a: ----- b: 89.23 c: 90.23 ** compared to pentacyclic heptamer ^[17,18]	S1, 15 min a,b: 89.55 89.86 c: 89.13 d,e,f: 97.21 97.53 98.24 a,b:c:d:e:f 1.9:2.1:1: 2.0:2.0:2.1 S2,15 min a,b: 89.47 89.76 c: 89.11 d,e,f: 97.19 97.54 98.24 a,b:c:d:e:f 2.1:1.9:1:1.9 1.9:1.7	S1, 45 min a,b: 89.48 89.8 c: 89.16 d,e,f: 97.22 97.58 98.28 a,b:c:d:e:f 1.8:1.8:1: 1.8:1.8:2.0 S1,45min,r.t.* a,b: 89.23 89.68 c: ----- d,e,f: 97.23 97.48 98.27 a,b:c:d:e:f calc.: Q2:Q3:Q4 4:24:05	S2, 45 min Q2: 87.94 88.41 89.31 Q3: 99.18 101 Q4: 101.09 101.35 Q2:Q3:Q4 4:23:9:5:0	S1, 45 min a,b: 98.67 c: 99.01 d: 88.66 (a+b):c:d 7.93:1.91:1

Figure 9. Assignment of ^{29}Si liquid NMR signals and comparison with literature data^{21–23} (negative signs of chemical shifts are omitted).

spectrum of Figure 4 further evidences the formation of several smaller species including the tricyclic hexamer (Figure 8) not present before. It is evident that the intense lines at $\delta = -98.67$ and -99.01 ppm in S1, 45 min (Figure 4) are caused by a species that is likely to be derived from the tetracyclic undecamer formed earlier (Figure 3). This species decomposes upon heating to room temperature into the double five-ring (Figure 5) and the observed smaller entities. The structure of the half-cagelike tetracyclic undecamer suggests the possibility to close it into a capped double five-ring. This species matches with the observed 8:2:1 intensity ratios of the $\delta = -98.67$, -99.01 , and -88.66 ppm signals. Heating to room temperature of this small cage results in removal of the capping silicon atom, which attaches itself to other siliceous species. For instance, the addition of one silicon atom to a bicyclic pentamer results in the formation of the tricyclic hexamer appearing together with the double five-ring (Figure 5). The capped double five-ring was discussed as a possible building unit in the formation of MFI.⁸ The present observation of its complete decomposition at room temperature, however, makes its involvement in the MFI crystallization process rather unlikely.

When TEOS and TPAOH solution are mixed at room temperature for 45 min, a totally different spectrum is recorded (S2, 45 min, Figure 7). The sample contains a small amount of Q^2 species and a large number of signals in the range between $\delta = -99$ and -102 ppm. This range usually is ascribed to branching Q^3 silicon atoms but can already contain Q^4 nuclei in the high shift region.²¹ Indeed, the broadening of the signals at $\delta = -101.09$ and -101.35 ppm makes the presence of Q^4 silicons highly probable. The rather high shift values for the Q^3 silicons disclaim the presence of double five-rings or four-rings and suggest the presence of a larger polyanion. The evolution of the IR spectrum to that of MFI type material after such time (Figure 1A) suggests the presence of a molecular fragment of this framework structure. Furthermore, this fragment should be related to the species detected after 15 min (S2, 15min). A ringlike particle formed by linking three tetracyclic undecamers ("trimer") satisfies all requirements. It is part of the MFI framework and has a $\text{Q}^2:\text{Q}^3:\text{Q}^4$ ratio which closely matches the measured intensity ratios of 4:24:5 (Figures 7 and 8). This 33 Si atom containing ring structure can accommodate a TPA cation with its hydrophobic alkyl chains, as envisioned in Figure 10 and derived from geometric considerations. Two

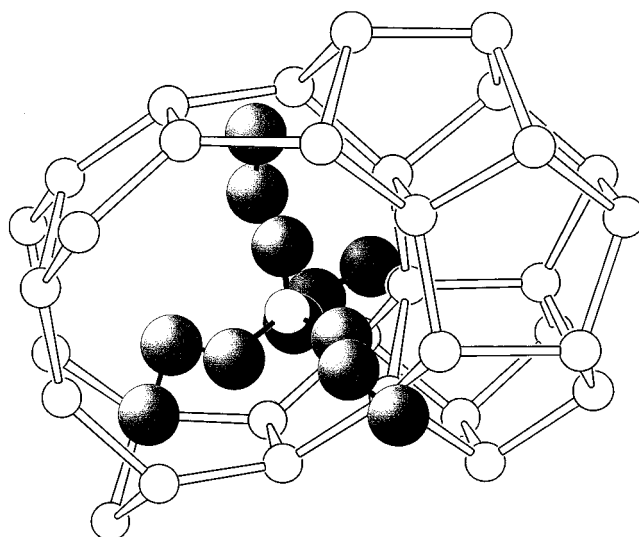


Figure 10. Structure of the ringlike "trimer" structure containing a TPA template molecule, as derived by geometric considerations.

of the four methyl groups can point into the two capped six-rings that are part of the channel segment, whereas the remaining two alkyl chains can embrace Q^4 silicon atoms in the blocklike attachment to the channel. In this configuration, the interaction of the propyl groups with dissociated silanols is minimized. This peculiar entity may be identified with the tetrapods proposed by Burkett and Davis.¹¹

Additional evidence for the presence of this 33 Si atom containing species can be gained from in situ X-ray scattering (XRS) and gel permeation chromatography (GPC).²⁴ The position of the XRS signal at $6.5^\circ 2\theta$ recorded after the mixing of TEOS with TPAOH correlates with a particle size of 1.3 nm, matching with the size of the proposed trimer. Furthermore, the observation of a comparatively sharp scattering band also favors the almost exclusive presence of a specific particle size. Thus, the conclusion that the signals recorded in the NMR spectrum S2, 45 min (Figure 7) arise from a single species is justified. Another observation is also of importance in this context. The step height of 1.3 nm observed by AFM during the study of the nanoslabs¹⁴ and the colloidal Silicalite-1 end product²⁰ matches the diameter of the trimer, hinting at its involvement in the formation of MFI-type material.

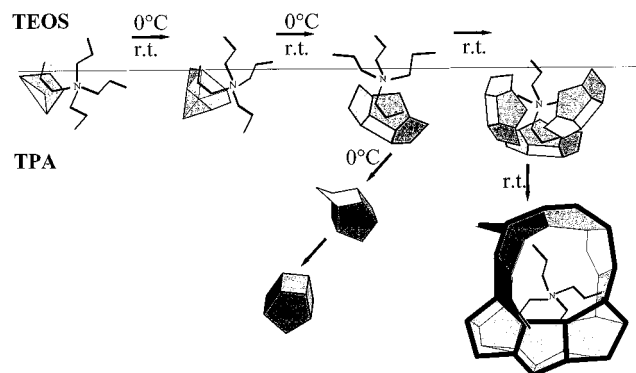


Figure 11. Schematic presentation of the TPA-directed polycondensation process of TEOS.

The TPA-Directed Silicon Polycondensation Process. The in situ IR and the NMR experiments give evidence for a directed silicon condensation process in concentrated solutions prepared from TEOS and aqueous TPAOH. Both methods point at the formation of only a few specific five- and three-ring containing species. The assignment of the NMR spectra gives insight into the condensation process depending on time and temperature. Up to 15 min, the temperature does not influence the reaction path (Figures 3 and 6). The formation of annealed five-ring species and the depletion of three-ring entities are observed by IR and NMR.

The nature of the observed silicate species suggests that the template functions as a structure directing agent even at these early stages. With the present data, it is possible to propose the following model for the TPA mediated silicon polycondensation process (Figure 11).

The key for understanding the successive steps is the hydrophobic surface of the propyl chains of the TPA, which tend to sheath in siliceous gloves,^{3,4,13,25,26} while the TPA cation as a whole strains for the charge compensation. The bicyclic pentamer, the pentacyclic octamer, and the tetracyclic undecamer represent a growing curved hydrophobic SiO₂ surface with all hydroxyl groups pointing outward. Thus, a bifunctional interface with an outer hydrophilic and an inner hydrophobic surface is created.

In the emulsions, TPAOH with its properties as a surfactant is located preferably at the liquid–liquid interface, with three of its propyl groups pointing into the TEOS layer. Thus, every TEOS molecule will encounter and pass an alkyl surface before hydrolysis in the aqueous phase (Figure 11). Therefore, it is probable that the structure direction by the template and the hydrolysis of the silicon source take place simultaneously.

The mixing of TPAOH and TEOS at room temperature results after 45 min in the formation of the “trimer” representing even a stronger pronunciation of this “glove” principle. At room temperature, the TPA molecule can mold three monomers (tetracyclic undecamers) into the observed ring structure, which can depart from the liquid–liquid interface as a whole and dissolve in the watery phase. It is noteworthy that this trimer is formed almost as the sole final product (Figure 7).

In the presence of alkaline cations²¹ or smaller tetraalkylammonium cations^{3,4} on the other hand, the observed species tend to a higher degree of internal condensation. They form rather small, closed cage-like structures, therewith presenting hydroxyl groups to the medium like a “hedgehog”. A similar phenomenon was observed after 45 min at 0 °C. The tetracyclic undecamer closes to form a capped double five-ring (Figure 4), which decomposes at room temperature into a pentagonal prism (Figure 5). These two “hedgehog” structures exposing a polar surface

do not interact with the TPA cation. A further difference between 0 °C and room temperature was the observation that after mixing for 45 min at 0 °C, a phase boundary between TEOS and TPAOH was still present, whereas at room temperature after the same time, all TEOS was hydrolyzed and transferred to the watery phase. It seems that at 0 °C, the tetracyclic undecamer departs from the interface into the aqueous layer. Lacking the intimate interaction with the TPA on its hydrophobic side, the released species has no choice but to condense internally in order to shield it from interaction with the aqueous surroundings. The TPA ions remain at the interface and repeat the tetracyclic undecamer formation. Indeed, some amount of the undecamer can be observed in S1, 45min (Figure 4). It is likely that the population is still bound to the TPA. The low amount of tetracyclic undecamer, furthermore, indicates that the closing mechanism takes place shortly after the release from the template. The sample at 0 °C thus resembles the situation in the presence of alkaline cations²¹ or tetramethylammonium cations^{3,4} in which the formation of the closed cage-like structures is also more favored.

The absence of pentagonal prisms in S2, 45 min indicates that during the trimerization of the tetracyclic undecamers, the contact to a template molecule is lost at no time. This suggests an aggregation mechanism, where all three of the monomers are interacting with propyl groups of the same TPA cation (Figure 10). Whether the absence of the “trimer” species at 0 °C in S1, 45 min is caused by the lack in activation energy or the failure of the template molecules to attach simultaneously three undecamers is still subject to discussion, but the latter explanation seems more probable. If it were just an activation problem, at least some “trimer” species should form after heating this sample to room temperature, which was not observed (S1, 45 min, r.t. Figure 5).

This study shows how TPAOH determines the kind of silicate species formed during the very first steps of the synthesis of MFI-type SiO₂ polymorphs in the system studied. The TPA molecule directs the formation of bicyclic pentamer, the pentacyclic octamer, the tetracyclic undecamer, and finally the trimer, representing a 33 Si atom containing MFI framework fragment. This sequence is in full accordance with the results of Kinrade et al. who proposed the larger template molecules to favor rather open polysilicate anions which can accommodate the templates.^{3,4}

The next question to be addressed is the mechanism of formation of the nanoslabs from this precursor. In the next paper,²⁴ we will present our observations of a step-by-step aggregation of the precursor species to result in the specific structure of the nanoslabs.

Acknowledgment. This work was sponsored by the Belgian Government in the frame of IUAP-PAI (postdoctoral fellowship to C.E.A.K.) and by the Flemish Fund for Scientific Research. P.J.G. acknowledges the same Fund for a research position. R.R. acknowledges K.U. Leuven for a postdoctoral fellowship.

References and Notes

- (1) Meier, W. M.; Olson, D. H.; Baerlocher, Ch. *Zeolites* **1996**, *17*, 1.
- (2) Flanigen, E. M. In *Proceedings of the Fifth International Conference on Zeolites*; L. V. Rees, H., Ed.; 1980, p 760.
- (3) Kinrade, S. D.; Knight, C. T. G.; Pole, D. L.; Syvitski, R. T. *Inorg. Chem.* **1998**, *37*, 4272.
- (4) Kinrade, S. D.; Knight, C. T. G.; Pole, D. L.; Syvitski, R. T. *Inorg. Chem.* **1998**, *37*, 4278.
- (5) Kokotailo, G. T.; Lawton, S. L.; Olson, D. H.; Meier, W. M. *Nature* **1978**, *272*, 437.

- (6) Flanigen, E. M.; Bennett, J. M.; Grose, R. W.; Cohen, J. P.; Patton, R. L.; Kirchner, R. M.; Smith, J. V. *Nature* **1978**, *271*, 512.
- (7) Engelhardt, G.; Hoebbel, D.; Tarmak, M.; Samoson, A.; Lippmaa, E. *Z. Anorg. Chem.* **1982**, *484*, 22.
- (8) Groenen, E. J. J.; Kortbeek, A. G. T. G.; Mackay, M.; Sudmeijer, O. *Zeolites* **1986**, *6*, 403.
- (9) Bell, A. T. In *Zeolite Synthesis*; Ocelli, M. L., Robson, H. E., Eds.; ACS Symposium Series 398; American Chemical Society: Washington, DC, 1998; p 66.
- (10) Gilson, J. P. *Zeolite Microporous Solids: Synthesis, Structure and Reactivity*; Derouane, Lemos, Nacchache, Ribeiro, Eds.; NATO ASI Series, 352; Kluwer Academic Publishers: Dordrecht, 1992; p 19.
- (11) Burkett, S. L.; Davis, M. E. *J. Phys. Chem.* **1994**, *98*, 4647.
- (12) Regev, O.; Cohen, Y.; Kehat, E.; Talmon, Y. *Zeolites* **1994**, *14*, 314.
- (13) Chang, C. D.; Bell, A. T. *Catal. Lett.* **1991**, *8*, 305.
- (14) Ravishankar, R.; Kirschhock, C. E. A.; Knops-Gerrits, P. P.; Feijen, E. J. P.; Grobet, P. J.; Vanoppen, P.; De Schryver, F. C.; Mieke, G.; Schoeman, B. J.; Jacobs, P. A.; Martens, J. A. *J. Phys. Chem. B* **1999**, *103*, 4960.
- (15) Perego, G.; Millini, R.; Perego, C.; Carati, A.; Pazzuconi, G.; Bellussi, C. *Stud. Surf. Sci. Catal.* **1997**, *105*, 205.
- (16) Flanigen, E. M.; Hassan, K.; Szymanski, H. A. *Adv. Chem. Ser.* **1971**, *101*, 201.
- (17) Flanigen, E. M. In *Zeolite Chemistry and Catalysis*; Rabo, J. A., Ed.; ACS Monograph Series 171; American Chemical Society: Washington, DC, 1976; p 80.
- (18) Jansen, J. C.; van der Gaag, F. J.; van Bekkum, H. *Zeolites* **1984**, *4*, 369–372.
- (19) Ravishankar, R.; Kirschhock, C.; Schoeman, B. J.; Vos, D. D.; Grobet, P. J.; Jacobs, P. A.; Martens, J. A. In *Proceedings of the 12th International Zeolite Conference*; Treacy, Marcus, Bisher, Higgins, Eds.; Material Research Society: Pennsylvania, 1999; Vol. III, p 1825.
- (20) Ravishankar, R.; Kirschhock, C.; Schoeman, B. J.; Vanoppen, P.; Grobet, P. J.; Storck, S.; Maier, W. F.; Martens, J. A.; De Schryver, F. C.; Jacobs, P. A. *J. Phys. Chem. B* **1998**, *102*, 2633.
- (21) Engelhardt, G.; Michel, D. *High-Resolution Solid-State NMR of Silicates and Zeolites*; John Wiley & Sons: New York, 1987.
- (22) Moravetski, V.; Hill, J. R.; Eichler, U.; Cheetham, A. K.; Sauer, J. *J. Am. Chem. Soc.* **1996**, *118*, 13015.
- (23) Harris, R. K.; Knight, C. T. *J. Chem. Soc., Faraday Trans. 2* **1983**, *79*, 1525 and 1539.
- (24) Kirschhock, C. E. A.; Ravishankar, R.; Van Looveren, L.; Jacobs, P. A.; Martens, J. A. *J. Phys. Chem. B* **1999**, *103*, 4972.
- (25) McMullan, R. K.; Bonamico, M.; Jeffrey, G. A. *J. Phys. Chem.* **1963**, *39*, 3295.
- (26) Weyl, H. S.; Marboe, E. C. *The Constitution of Glasses*; Wiley: New York, 1967; Vol. 2, p 1480.